Pergamon

Tetrahedron: Asymmetry, Vol. 8, No. 12, pp. 2069–2073, 1997

Printed in Great Britain
PII: S0957-4166(97)00216-4
0957-4166/97 $17.00 + 0.00

Enantiomerization barriers by dynamic HPLC. Stationary phase effects

Francesco Gasparrini, Domenico Misiti, Marco Pierini* and Claudio Villani* *
Dipartimento di Studi di Chimica e Tecnologia delle Sostanze Biologicamente Attive, Università 'La Sapienza', P. le A. Moro 5, 00185 Roma, Italy

Abstract: Chiral atropisomeric naphthamides have been used as model compounds to investigate solute interconversion phenomena in free solution and during liquid chromatography on a chiral stationary phase; energy barriers measured in the mobile phase (thermal racemization of enriched samples) are 0.3–1.3 Kcal/mol lower than those measured in the stationary phase (computer simulation). © 1997 Elsevier Science Ltd

Introduction

Chiral compounds with stereolabile units can be conveniently investigated by Dynamic High Performance Liquid Chromatography (DHPLC) on a chiral stationary phase (CSP), either in the form of variable temperature or variable flow chromatography.[1] During a DHPLC experiment the column acts simultaneously as a 'chemical reactor' and a separation device: first-order, reversible $R \rightleftharpoons S$ processes (enantiomerizations) where the interconversion rates are on the same time scale as the column separation rate, produce temperature and flow dependent chromatographic profiles, with an interference regime (plateau) between the *R* and *S* resolved peaks. We have detected such peak deformations during HPLC on brush-type CSPs for a range of stereolabile chiral compounds[2–7] with different energy barriers ($\Delta G^{\#}$) spanning about 10 Kcal/mol. Computer simulation of the experimentally observed elution profile has been recently used to obtain overall rate constants for the enantiomerization process during HPLC[8] and GC[9] on chiral phases. These rate constants are averaged values that bring contributions from the process occurring in the mobile phase (k_m) and in the stationary phase (k_s); if one of the two constants (usually k_m) is available from independent measurements, the missing rate constant can be obtained by simulation.[9a] Here we describe the dynamic chromatographic behaviour of chiral atropisomeric 2-substituted naphthamides **1–4**, whose enantiomers are separated on the brush-type chiral stationary phase (3*R*,4*S*)-Whelk-O1 (Scheme 1); the stationary phase influence on the enantiomerization rate constants is studied by combining the results from free solution thermal racemization of preparatively enriched samples and from computer simulation of experimental chromatograms featuring peak deformations due to on-column $R \rightleftharpoons S$ interconversion.

Results and discussion

Naphthamides **1–4** adopt a conformation in which the carboxamide group is twisted with respect to the naphthyl ring; hindered rotation around the C_{Ar}–CO bond thus allows for the existence of conformational enantiomers whose enantiomerization barriers are large enough ($\Delta G^{\#}$ >21 Kcal/mol) to enable their physical separation by HPLC.[10] During chromatography of these compounds on **CSP1** at room temperature the enantiomerization process occurs at a lower rate than the separation process (slow exchange) and the chromatographic profiles are unaffected by the $R \rightleftharpoons S$ stereomutation equilibrium; however, as the two rates were made to approach each other (e.g. by raising the column temperature, T_{col}, or by decreasing the eluent flow rate, ϕ), we observed the inset of peak deformations due to on-column enantiomerization. We systematically varied T_{col} and ϕ to obtain chromatograms

* Corresponding author. Email: villani@axrma.uniroma1.it

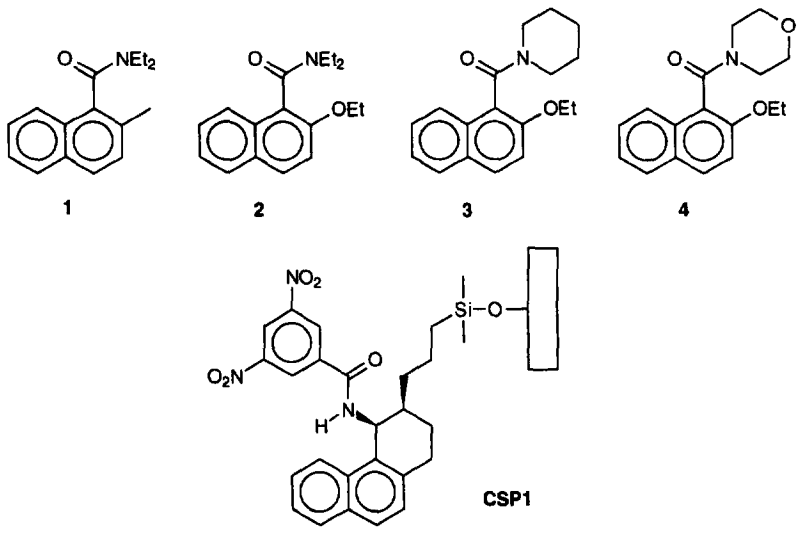

Scheme 1.

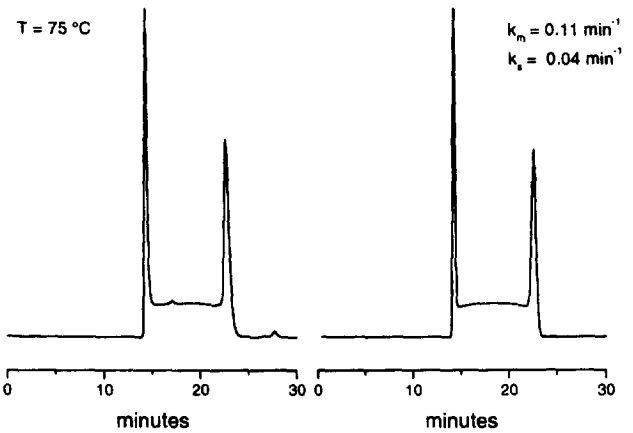

Figure 1. Experimental (left) and simulated chromatograms with input parameters (right) of **1** on **CSP1**. UV detection at 280 nm. Other experimental conditions as in Table 1.

featuring a visible plateau and symmetrical peak shapes; next we isolated by semipreparative HPLC the individual enantiomers and determined the enantiomerization rate constants k_m (and the associated energy barriers, $\Delta G^{\#}_m$) in a batch reactor at the same temperature (T_{col}) and in the same solvent used for the dynamic HPLC runs; finally we used these rate constants as fixed input parameters for the computer simulations (Figure 1) which yielded both the apparent rate constants (k_{app1} and k_{app2}, sum of rate constants in the mobile and stationary phases weighted by the time each enantiomer is present in each phase, see equations (a) and (b) in ref.[8a]) and the rate constants in the stationary phase k_{s1} and k_{s2}; the corresponding energy barriers[11] are listed in Table 1.

As shown, the enantiomerization process is always faster in free solution than in the stationary phase; the differences between the energy barriers in the two phases increase with retention of the analytes, and are in the range 0.3–0.7 and 1.0–1.3 Kcal/mol for the first and second eluted enantiomers, respectively. These figures are consistent with the interactions involved in the enantiorecognition process operated by the Whelk-O1 phase for our compounds, i.e. one H-bond interaction between the analyte carbonyl

Table 1.

comp.	K'_1[a]	K'_2[a]	T (°C)[b]	flow rate[c]	$\Delta G^{\#}_m$[d]	$\Delta G^{\#}_{s1}$[e]	$\Delta G^{\#}_{s2}$[e]	$\Delta G^{\#}_{app1}$[e]	$\Delta G^{\#}_{app2}$[e]
1	1.95	3.69	75	0.5	24.80	25.34	25.78	25.12	25.44
2	2.12	5.62	65	0.5	23.79	24.10	24.76	23.96	24.46
3	10.34	28.65	45	1.0	22.34	23.04	23.68	22.91	23.52
4	7.05	22.53	45	2.0	21.91	22.25	22.99	22.17	22.85

[a] capacity factors for the 1st and 2nd eluted enantiomers defined as $K = (t-t_0)/t_0$; eluent: hexane/*i*-propanol 80/20.
[b] column temperature for the DHPLC runs and temperature for the off-column thermal racemization experiments.
[c] eluent flow rate in ml/min.
[d] energy barriers (in Kcal/mol, ± 0.1%) from off-column thermal racemization in heptane/*i*-propanol 80/20.
[e] energy barriers (in Kcal/mol, ± 0.2%) from computer simulation.

oxygen and the CSP amide N–H and aromatic–aromatic interactions between the analyte naphthyl ring and the 3,5-dinitrobenzoyl and naphthyl rings of the CSP:[10] clearly, the $R \rightleftharpoons S$ interconversions of **1–4** in the adsorbed state are somehow inhibited compared to the free solution since at least one of the above interactions must be weakened or completely lost to allow for the analyte internal motions. Averaged values of $\Delta G^{\#}_s$ for the first and second eluted enantiomers of **1–4** are 0.6–1.0 Kcal/mol greater than the corresponding $\Delta G^{\#}_m$; thus, the inhibitory effects of the CSP are similar in magnitude to those recorded by NMR for some related, H-bonded systems: for example, the chiral solvating agents trifluoromethylphenyl- and trifluoromethylanthrylcarbinols raise the enantiomerization barriers of an atropisomeric N-nitrosamine[12] and of a naphthyl ketone[7] by 0.7 and 0.5 Kcal/mol, respectively.

If the rate constants in the mobile phase are not available, only the apparent rate constants obtained by simulation (and the associated energy barriers, $\Delta G^{\#}_{app1,2}$ in Table 1) are meaningful, since several combinations of input parameters (k_m and k_s) will equally reproduce the experimental chromatograms. Inspection of the energy barriers calculated for **1–4** from the apparent rate constants shows that they exceed $\Delta G^{\#}_m$ by 0.2–1.2 Kcal/mol; if the apparent energy barriers for the first and second eluted enantiomers are averaged, the differences between the averaged values and $\Delta G^{\#}_m$ amount to 0.4–0.9 Kcal/mol. Since computer simulation alone gives only apparent rate constants, a preliminary estimate of the magnitude and direction (activating or deactivating) of the stationary phase effects on isomerization rates is required when k_m values are not available; although our results were generated from a small set of compounds with little functional groups variations, we believe that similar stationary phase effects (increase of isomerization barriers by 0.5–1.0 Kcal/mol) are to be expected for other solute/CSP combinations in which retention is driven by H-bonding and aromatic–aromatic interactions.

Experimental

^1H and ^{13}C NMR spectra were recorded on a Bruker AM 200 spectrometer at 200 and 50.3 MHz, respectively, in $CDCl_3$, unless otherwise stated; chemical shifts are reported in ppm downfield to internal TMS. FT-IR were recorded on a Nicolet 5DX instrument. Room temperature HPLC was performed as described.[13] Variable temperature HPLC was performed by placing the column inside a GC oven (ΔT ±0.1°C); thermal equilibration of the eluent was obtained through a 50 cm capillary, connecting the injector and the column, placed inside the oven. The (3*R*,4*S*)-Whelk-O1 column[14] (250×4.6 mm I.D.) was obtained from Regis Technologies Inc., Morton Grove, IL 60053, USA.

Compounds **1–4** were prepared from the corresponding acid chlorides and the appropriate amine and identified as follows.

N,N-*Diethyl-2-methyl-1-naphthalenecarboxamide 1*

Oil, FT-IR (liquid film): 1630 cm^{-1}; ^1H NMR δ: 7.80–7.66 (m, 3H), 7.38–7.31 (m, 3H), 3.88–3.56 (m, 2H), 3.04 (q, *J*=7.1 Hz, 2H), 2.42 (s, 3H), 1.37 (t, *J*=7.1 Hz, 3H), 0.90 (t, *J*=7.1 Hz, 3H); ^{13}C

NMR δ: 169.65, 133.11, 131.56, 130.97, 129.58, 128.18, 127.96, 127.81, 126.51, 125.18, 124.23, 42.50, 38.50, 19.14, 13.80, 12.77. Anal. Calcd. for $C_{16}H_{19}NO$: C, 79.63; H, 7.94; N, 5.80. Found: C, 79.90; H, 7.89; N, 5.77.

N,N-*Diethyl-2-ethoxy-1-naphthalenecarboxamide* **2**

M.p. 72–73°C; FT-IR (KBr): 1626 cm^{-1}; ^1H NMR δ: 7.83–7.63 (m, 3H), 7.48–7.21 (m, 3H), 4.19 (q, *J*=7.0 Hz, 2H), 3.90–3.55 (m, 2H), 3.19–3.07 (m, 2H), 1.41 (t, *J*=7.0 Hz, 3H), 1.36 (t, *J*=7.1 Hz, 3H), 0.96 (t, *J*=7.1 Hz, 3H); ^{13}C NMR δ: 167.91, 151.83, 131.09, 129.94, 128.86, 127.91, 127.15, 123.98, 123.94, 120.99, 114.19, 64.84, 42.76, 38.74, 15.02, 14.06, 12.89. Anal. Calcd. for $C_{17}H_{21}NO_2$: C, 75.25; H, 7.80; N, 5.16. Found: C, 75.52; H, 7.76; N, 5.13.

1-[(2-Ethoxy-1-naphthalenyl)-carbonyl]-piperidine **3**

M.p. 101–102°C; FT-IR (KBr): 1622 cm^{-1}; ^1H NMR δ: 7.84–7.65 (m, 3H), 7.48–7.22 (m, 3H), 4.20 (q, *J*=7.0 Hz, 2H), 3.90 (m, 2H), 3.15 (m, 2H), 1.73–1.63(m, 4H), 1.42 (t, *J*=7.0 Hz, 3H) overlapped with a 2H multiplet, splitted in two 1H multiplets (δ 1.51 and 1.38) at 500 MHz; ^{13}C NMR δ: 166.99, 151.89, 130.90, 130.12, 128.77, 127.92, 127.20, 123.95, 123.92, 120.02, 114.02, 64.76, 47.74, 42.54, 26.53, 25.84, 24.61, 15.07. Anal. Calcd. for $C_{18}H_{21}NO_2$: C, 76.30; H, 7.47; N, 4.94. Found: C, 76.57; H, 7.45; N, 4.91.

4-[(2-Ethoxy-1-naphthalenyl)-carbonyl]-morpholine **4**

M.p. 114–115°C; FT-IR (KBr): 1636 cm^{-1}; ^1H NMR δ: 7.85 (d, *J*=9.0 Hz, 1H), 7.81–7.66 (m, 2H), 7.52–7.32 (m, 2H), 7.25 (d, *J*=9.0 Hz, 1H), 4.29–4.15 (m, 2H), 4.00–3.94 (m, 2H), 3.88–3.81 (m, 2H), 3.69–3.46 (m, 2H), 3.34–3.12 (m, 2H) 1.45 (t, *J*=7.0 Hz, 3H); ^{13}C NMR δ: 167.24, 151.97, 130.90, 130.57, 128.79, 128.03, 127.50, 124.13, 123.73, 119.08, 113.77, 67.17, 66.99, 64.76, 46.93, 41.99, 15.10. Anal. Calcd. for $C_{17}H_{19}NO_3$: C, 71.56; H, 6.71; N, 4.91. Found: C, 71.77; H, 6.69; N, 4.90.

Off-column racemization experiments. About 10 mg of racemic material was resolved on the analytical Whelk-O1 column (≈3 mg per run) using CH_2Cl_2/hexane mixtures as eluent; the first eluted fractions, with e.e. >98%, were evaporated at 10–15°C and stored at −23°C until used in the racemization experiments: about 3 mg of enriched sample was dissolved in 200 μl of *i*-propanol and immediately added via syringe to a thermostated vessel containing 4 ml of heptane/*i*-propanol 80/20; variation of e.e. with time was monitored by sampling 20 μl of the mixture, quenching with 200 μl of cooled (5°C) eluent and HPLC analysis on the Whelk-O1 column (eluent: hexane/*i*-propanol/MeOH 70/30/10, T=20°C, UV detection at 280 nm; no on-column interconversion detected under these conditions); enantiomerization rate constants (k_m in the text) were obtained from the relationship[15] $k_{(racemization)}=2k_{(enantiomerization)}$.

Simulations of experimental chromatograms were performed with the SIMUL[16] program modified by one of the authors (M. P.): the modified program, running on a personal computer (FORTRAN77), accepts experimental chromatograms in ASCII format, allows on-screen comparison with the simulated chromatograms and directly returns $k_{s1,2}$, $k_{app1,2}$ and the associated energy barriers.

Acknowledgements

This work was performed with financial support from MURST and CNR.

References

1. Gasparrini, F.; Lunazzi, L.; Misiti, D.; Villani, C. *Acc. Chem. Res.* **1995**, *28*, 163 and references cited therein.
2. Casarini, D.; Foresti, E.; Gasparrini, F.; Lunazzi, L.; Misiti, D.; Macciantelli, D.; Villani, C. *J. Org. Chem.* **1993**, *58*, 5674.
3. Casarini, D.; Cirilli, M.; Gasparrini, F.; Gavuzzo, E.; Lunazzi, L.; Villani, C. *J. Org. Chem.* **1995**, *60*, 97.
4. Villani, C.; Pirkle, W. H. *Tetrahedron: Asymmetry* **1995**, *6*, 27.

5. Alcaro, S.; Casarini, D.; Gasparrini, F.; Lunazzi, L.; Villani, C. *J. Org. Chem.* **1995**, *60*, 5515.
6. Gasparrini, F.; Misiti, D.; Villani, C. *J. Chromatogr. A* **1995**, *694*, 163.
7. Casarini, D.; Lunazzi, L.; Pasquali, F.; Gasparrini, F; Villani, C. *J. Am. Chem. Soc.* **1992**, *114*, 6521.
8. a) Veciana, J.; Crespo, M. I. *Angew. Chem., Int. Ed. Engl.* **1991**, *30*, 74; b) Stephan, B.; Zinner, H.; Kastner, F.; Mannschreck, A. *Chimia* **1990**, *44*, 336; c) Friary, R. J.; Spangler, M.; Osterman, R.; Schulman, L.; Schwerdt, J. H. *Chirality* **1996**, *8*, 364; d) Cabrera, K.; Jung, M.; Fluck, M.; Schurig, V. *J. Chromatogr. A* **1996**, *731*, 315.
9. a) Jung, M.; Schurig, V. *J. Am. Chem. Soc.* **1992**, *114*, 529; b) Schurig, V.; Jung, M.; Schleimer, M.; Klarner, F.-G. *Chem. Ber.* **1992**, *125*, 1301; c) Wolf, C.; Hochmuth, D. H.; König, W. A.; Roussel, C. *Liebigs. Ann. Chem.* **1996**, 357.
10. a) Cuyegkeng, M.; Mannschreck, A. *Chem. Ber.* **1987**, *120*, 803; b) Pirkle, W. H.; Welch, C. J.; Zych, A. J. *J. Chromatogr.* **1993**, *648*, 101; c) Bowles, P.; Clayden, J.; Tomkinson, M. *Tetrahedron Lett.* **1995**, *36*, 9219.
11. Here we focus on the differences between $\Delta G^{\#}_{m}$ and $\Delta G^{\#}_{s}$ for **1–4**; we make no attempt to interpret energy barriers in terms of sequential or correlated Ar–CO rotation (HPLC visible on a CSP) and CO–N rotation (HPLC invisible for **1–4**).
12. Lefèvre, F.; Burgemeister, T.; Mannschreck, A. *Tetrahedron Lett.* **1977**, 1125.
13. Gasparrini, F.; Misiti, D.; Pierini, M.; Villani, C. *J. Chromatogr. A* **1996**, *724*, 79.
14. The configurational description of the commercial (*S,S*)-Whelk-O1 phase (used in this study) has been revised and corrected to (3*R*,4*S*); see: Pirkle, W. H.; Brice, L. J.; Widlanski, T. S.; Roestamadji, J. *Tetrahedron: Asymmetry* **1996**, *7*, 2173.
15. Eliel, E. L.; Wilen, S. H. *Stereochemistry of Organic Compounds* John Wiley and Sons, New York, 1994, p. 426.
16. Jung, M. *QCPE Bull.* **1992**, 12, 52.

(Received in UK 16 April 1997)